Available online at www.sciencedirect.com
SCIENCE DIRECT
Trans. Nonferrous Met. Soc. China 16(2006) 1268−1273
Transactions of Nonferrous Metals Society of China
www.csu.edu.cn/ysxb/

Simulation on function mechanism of T1(Al_2CuLi) precipitate in localized corrosion of Al-Cu-Li alloys

LI Jin-feng(李劲风), ZHENG Zi-qiao(郑子樵), REN Wen-da(任文达),
CHEN Wen-jing(陈文敬), ZHAO Xu-shan(赵旭山), LI Shi-chen(李世晨)

School of Materials Science and Engineering, Central South University, Changsha 410083, China

Received 1 March 2006; accepted 28 August 2006

Abstract: To clarify the corrosion mechanism associated with the precipitate of T1(Al_2CuLi) in Al-Li alloys, the simulated bulk precipitate of T1 was fabricated through melting and casting. Its electrochemical behavior and coupling behavior with α(Al) in 3.5% NaCl solution were investigated. Meanwhile, the simulated Al alloy containing T1 particle was prepared and its corrosion morphology was observed. The results show that there exists a dynamic conversion corrosion mechanism associated with the precipitate of T1. At the beginning, the precipitate of T1 is anodic to the alloy base and corrosion occurs on its surface. However, during its corrosion process, its potential moves to a positive direction with immersion time increasing, due to the preferential dissolution of Li and the enrichment of Cu. As a result, the corroded T1 becomes cathodic to the alloy base at a later stage, leading to the anodic dissolution and corrosion of the alloy base at its adjacent periphery. It is suggested that the localized corrosion associated with the precipitate of T1 in Al-Li alloys is caused by the alternate anodic dissolution of the T1 precipitate and the alloy base at its adjacent periphery.

Key words: Al-Cu-Li alloy; localized corrosion; mechanism; T1(Al_2CuLi) precipitate

1 Introduction

Al-Li alloys, compared with traditional Al alloys, possess more excellent properties, such as lower density, greater elastic modulus and higher specific strength. In the near future, they would be widely applied in airplane structures. However, they are susceptible to localized corrosion in moist environment. So it is important to investigate their corrosion behavior for their application.

A substantial amount of research work has been done for the corrosion behaviors of Al-Li alloys[1−4]. However, there still exist different viewpoints on the function mechanism of precipitates in localized corrosion of Al-Li alloys. As to the localized corrosion mechanism of the Al-Li alloys containing the precipitate of T1, there once have been two opposite viewpoints. According to the electrochemical behavior of simulated bulk T1, BUCHHEIT et al[5,6] thought that the intergranular corrosion(IGC) or intersubgranular corrosion(ISGC) of 2090 Al-Li alloy in NaCl solution was caused by the anodic dissolution of T1 precipitate. However, according to the corrosion morphologies, KUMAI et al[7] suggested that the preferential dissolution of precipitate-free zone(PFZ) along grain boundaries caused its intergranular corrosion in NaCl solution.

T1 is the main strengthening precipitate in some 2××× series Al-Li alloy, such as 2090 alloy and 2195 alloy, which precipitates preferentially at dislocations, subgrain boundaries and grain boundaries. During its precipitation, a Cu and Li-depleted precipitate-free zone(PFZ) is formed along grain boundary and subgrain boundary[8,9]. To clarify the functions of the aging precipitate of T1 in Al-Li alloys, its electrochemical behavior must be known and the corrosion morphology associated with it should be clearly distinguished. However, the aging precipitate of T1 in Al-Li alloys is very fine, and the corrosion morphologies associated with it can not be clearly observed by scanning electron microscope(SEM). In this paper, to understand the electrochemical behavior of the aging precipitate of T1, its simulated bulk phase was fabricated through melting and casting according to its chemical proportion. Its electrochemical behavior and coupling behavior with

Foundation item: Project(50401012) supported by the National Natural Science Foundation of China
Corresponding author: LI Jin-feng; Tel: +86-731-8830270; E-mail: lijinfeng@mail.csu.edu.cn

α(Al) were investigated. Meanwhile, a simulated Al alloy containing T1 particle was manufactured from α(Al) and the broken simulated T1 precipitate, and its corrosion morphology was observed by SEM.

2 Experimental

2.1 Preparation of simulated bulk precipitate of T1

The simulated bulk precipitate of T1 was manufactured through melting and casting. The cast ingot was annealed at 270 ℃ for 24 h and identified through X-ray diffraction(XRD). The PFZ or the alloy base is substituted by α(Al), due to its little alloying element.

The specimens for electrochemical measurement were cut form α(Al) and the simulated bulk precipitate of T1, connected to a copper wire, then mounted in epoxy resin with a surface exposed. The exposed surface was ground using abrasive papers through 500-grade to 1200-grade, polished with Cr_2O_3 powder, rinsed using acetone, degreased with distilled water and then dried in air. The corrosion medium was neutral 3.5% NaCl solution prepared using analytical NaCl and distilled water.

2.2 Coupling behavior and corrosion morphology of T1-α(Al) coupled system

The potentiodynamic scanning curves of individual α(Al) and the simulated precipitate of T1 were measured with a SI 1287 Electrochemical Interface in a three-compartment cell. The working electrode was α(Al) and the simulated T1 precipitate respectively. A large platinum sheet and saturated calomel electrode(SCE) with a Luggin capillary served as counter and reference electrodes, respectively. During the potentiodynamic scanning curve measurement, the cathodic polarization was carried out firstly, and then the anodic polarization, and the scanning rate was 1 mV/s.

Meanwhile, the simulated T1 precipitate and α(Al) were coupled in the NaCl solution with areas of T1 of 0.07 cm^2 and α(Al) of 0.13 cm^2, as seen in Fig.1. During the coupling process, the coupling current of T1-α(Al) was measured. 10 d later, the coupling test was finished, the coupled electrodes were disconnected, and the open circuit potential of corresponding electrode was measured with the SI 1287 Electrochemical Interface. The corrosion morphologies of the coupled electrodes were observed with a KYKY 2800 scanning electron microscope(SEM).

2.3 Corrosion of Al-Cu-Li alloy at beginning of immersion

To observe the corrosion associated with T1 precipitate at the beginning of corrosion, TEM samples

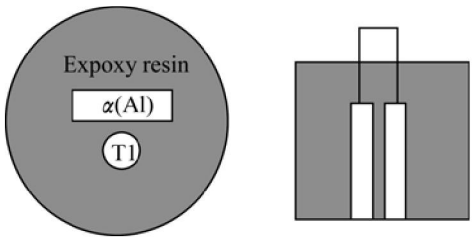

Fig.1 Schematic diagram of coupling system

of a 2195 Al-Li alloy, a kind of Al-Cu-Li alloys, were prepared. To clearly distinguish the corrosion associated with the T1 precipitate using a transmission electron microscope(TEM), the 2195 Al-Li alloy was aged at 300 ℃ for 24 h after solution treatment at 504 ℃ for 45 min and quenching in cold water. The objective of high aging temperature is to obtain coarse T1 precipitate.

The TEM samples were prepared using the twin-jet solution of 75% CH_3OH and 25% HNO_3. A sample was observed with a Tecnai G^2 TEM to obtain its microstructure. Another sample was immersed in the prepared NaCl solution for 1 h, and then observed with the Tecnai G^2 TEM.

2.4 Preparation of simulated Al alloy containing T1 particle and its corrosion morphology

The corrosion morphology associated with the precipitate of T1 can not been recognized by SEM due to its too small size in Al-Li alloys. To clearly observe the corrosion morphology associated with it, a simulated Al alloy containing T1 particle was made from α(Al) and the simulated precipitate of T1. Two α(Al) plates with a thickness of 5 mm were polished and cleaned using 50 g/L NaOH solution at 70 ℃. The broken simulated precipitates of T1 were placed between them, then they were laminated to 3 mm at 410 ℃, as shown in Fig.2. Then the laminated plate was annealed at 350 ℃ for 4 h. As a result, a simulated Al alloy containing T1 particles was formed.

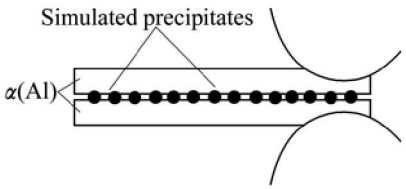

Fig.2 Simulated alloy process through rolling

The sectional surface of the simulated Al alloy was ground using abrasive papers through 500-grade to 1200-grade, polished with Cr_2O_3 powder, rinsed using acetone, degreased with distilled water and then dried in air. Then it was immersed in the prepared NaCl solution for 12 h. To clearly distinguish the corrosion morphology

of the simulated alloy, the corrosion product covered on the surface was removed using 2%CrO_3+5%H_3PO_4 solution at 80 ℃, and the corresponding corrosion morphology was observed by a KYKY 2800 SEM.

3 Results and discussion

Fig.3 shows the XRD pattern of the annealed ingot corresponding to the chemical proportion of T1. It is clearly seen that T1 is the main phase in the ingot, and there only exists a small quantity of θ and $T_B(Al_7Cu_4Li)$. The simulated T1 could be substituted for the real aging precipitate of T1 in Al-Li alloy to undergo electrochemical measurement. Meanwhile, the PFZ or the alloy base could be substituted by α(Al), due to its little alloying element.

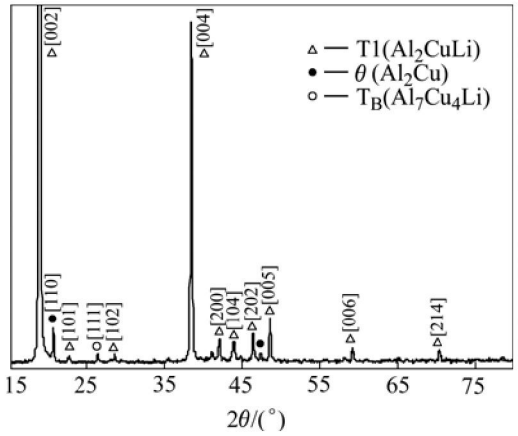

Fig.3 XRD pattern of ingot corresponding to chemical proportion of T1

The potentiodynamic scanning curves and corresponding corrosion parameters of individual α(Al) and the simulated T1 precipitate are presented in Fig.4 and Table 1 respectively. It is clearly seen that the corrosion potential(φ_{corr}) of T1 is negative with respect to that of α(Al). The polarization resistance(R_P) of T1 is much less than that of α(Al). Meanwhile, the corrosion current density(J_0) of T1 is much greater than that of α(Al), indicating that T1 is more susceptible to corrosion at the beginning.

Table 1 Corrosion parameters of α(Al) and T1 in 3.5% NaCl solution

Phase	φ_{corr} (vs SCE)/V	J_0/(A·cm^{-2})	R_p/(Ω·cm^2)
T1	−1.076	1.02×10^{-4}	254.2
α(Al)	−0.855	9.0×10^{-6}	2 897.7

After coupling for 10 d, the open circuit potential order of α(Al) and the simulated T1 precipitate changes. Compared with that at the beginning, the potential of T1 moves to a positive direction, resulting in the phenomenon that the potential of the simulated T1 precipitate becomes positive with respect to that of α(Al) at a later stage, as shown in Fig.5.

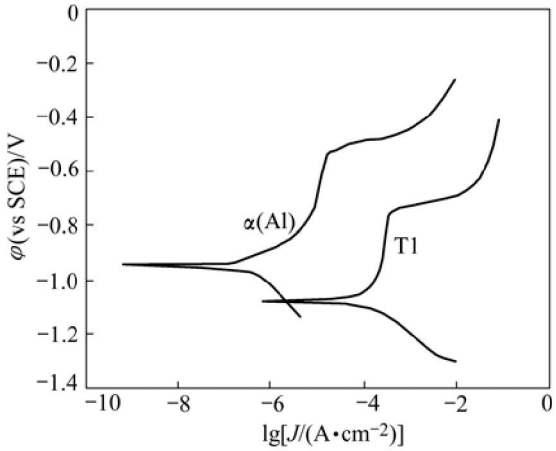

Fig.4 Potentiodynamic scanning curves of individual T1 and α(Al) in 3.5% NaCl solution

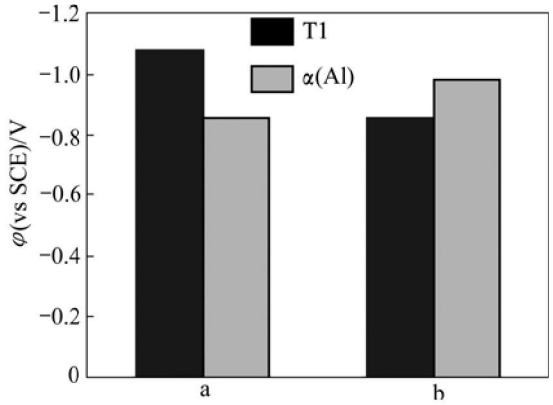

Fig.5 Open circuit potential variation of T1 and α(Al): (a) At beginning; (b) After coupling for 10 d

That the potential of T1 precipitate moves towards the positive direction can be explained by the preferential dissolution of Li from T1. The preferential dissolution phenomenon was also found in S(Al_2CuMg) particle in 2024 Al alloy and Mg_2Si particle in 6××× series Al alloy, which contain active element of Mg. BUCHHEIT et al [10], ZHU et al[11], SHAO et al[12] and LI et al[13] found that as 2××× series Al alloy containing S(Al_2CuMg) particle was immersed in NaCl solution, active Mg was preferentially dissolved, resulting in Cu-rich remnants. When 6××× series Al alloy was pickled in 0.1 mol/L phosphoric acid (pH=1.6), Mg is preferentially dissolved, resulting in Si-rich remnants in the Mg_2Si particle[14]. Like Mg, Li also possesses high chemical activity. Although the content of Li cannot be detected with EDAX, it should be rational to deduce that Li will be preferentially dissolved. In this case, the preferential dissolution of Li from T1 will lead to the enrichment of noble Cu. As a result, it is reasonable to

deduce that the potential of corroded T1 will move to the positive direction.

The potential change will cause the coupling current variation. Fig.6 shows the coupling current of T1-α(Al) system. At the initial immersion stage of 25 h, T1 endures anodic current in the coupling system. As immersion time increases and the potential of T1 becomes positive with respect to that of α(Al), the anodic current of T1 changes to cathodic current and increases.

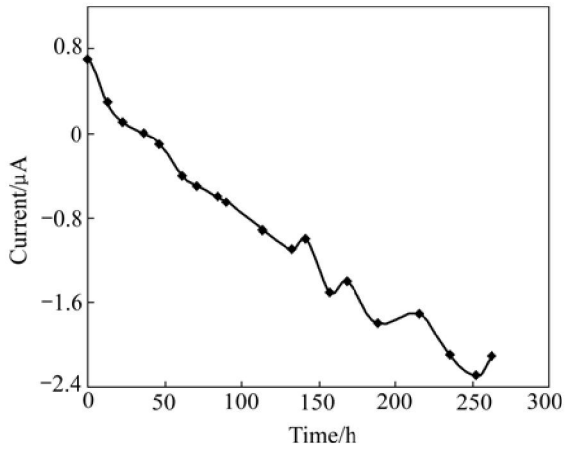

Fig.6 Coupling current of T1 in T1-α(Al) system

Fig.7 displays the morphologies of α(Al) after coupling with the simulated T1 precipitate in 3.5% NaCl solution for 10 d. Severe pitting corrosion is observed on α(Al) (seen in Fig.7(a)). Meanwhile, small pits are also found, which are connected to each other, as shown in Fig.7(b). To illustrate the corrosion degree of α(Al) coupled with the simulated T1 precipitate, an individual α(Al) without coupling was also immersed in the NaCl solution for 10 d, and its corrosion morphology was observed with the KYKY 2800 SEM. Compared with the corrosion morphology of α(Al) without coupling (see Fig.8), it can be found that the corrosion of α(Al) coupled with the simulated bulk T1 precipitate is more severe. That is to say, as the potential of corroded simulated T1 precipitate becomes positive with respect to that of α(Al) at a later stage of coupling, α(Al) endures anodic current and its corrosion is accelerated.

Fig.9(a) shows the bright field TEM micrograph of a 2195 Al-Li alloy. The size of the precipitate of T1 in this case is much bigger than that in the alloy aged at 180 ℃[15], due to its high aging temperature of 300 ℃. It is clearly seen that the color of T1 is darker than that of the alloy base at its periphery. The micrograph of another 2195 Al-Li alloy TEM sample immersed in 3.5% NaCl solution for 1 h is shown in Fig.9(b). It is found that the color of T1 is changed to white, being opposite to its original color. The color variation indicates that the precipitate of T1 in the 2195 Al-Li alloy is preferentially

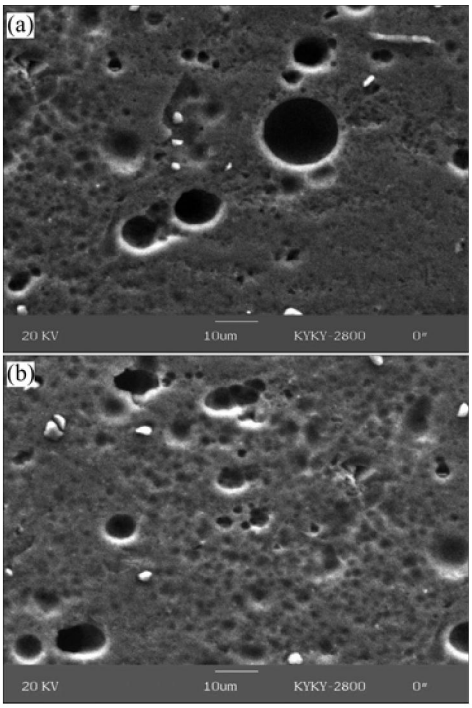

Fig.7 Corrosion morphologies of α(Al) coupled with simulated T1 precipitate in 3.5% NaCl solution for 10 d

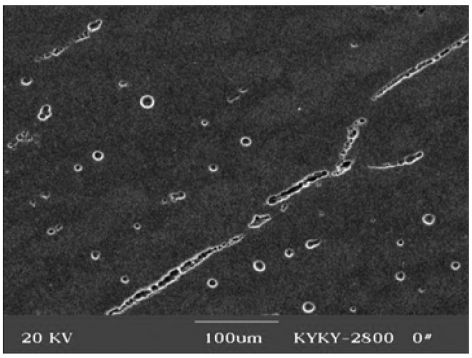

Fig.8 Corrosion morphology of individual α(Al) immersed in 3.5% NaCl solution for 10 d

corroded at the beginning of immersion. The preferential corrosion of the T1 precipitate in 2195 Al-Li alloy is caused by the potential difference between the alloy base (or α(Al)) and the T1 precipitate. It is found that the potential of the T1 precipitate is negative with respect to α(Al) at the beginning (see in Fig.4). So, as the alloy is immersed in NaCl solution, the precipitate of T1 acts as an anodic zone and is preferentially attacked at the beginning. While, the alloy base at its adjacent periphery is protected as a cathodic zone.

Fig.10 shows the original optical micrograph of the simulated Al alloy. The simulated T1 particle is surrounded by α(Al) and no obvious crevice is found between α(Al) and the simulated T1 particle. The corrosion morphology of the simulated Al alloy immersed in the NaCl solution for 12 h is presented in

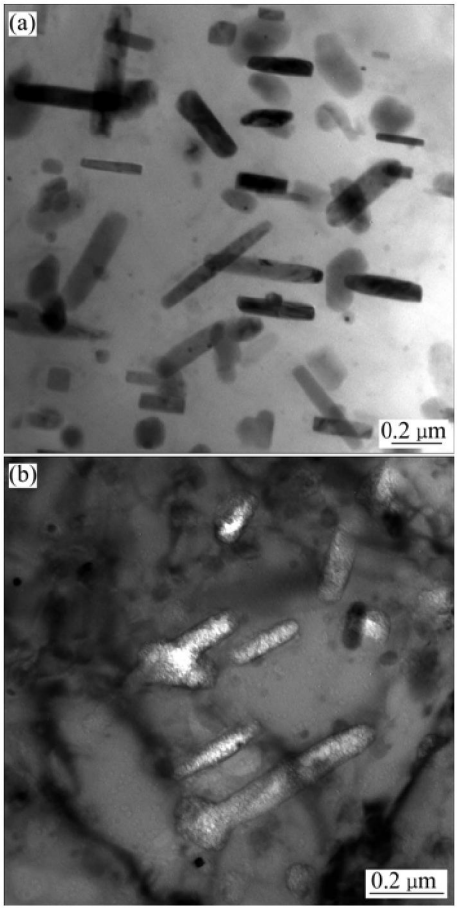

Fig.9 Micrographs of 2195 Al-Li alloy TEM sample: (a) Original; (b) After 1 h of immersion in 3.5% NaCl solution

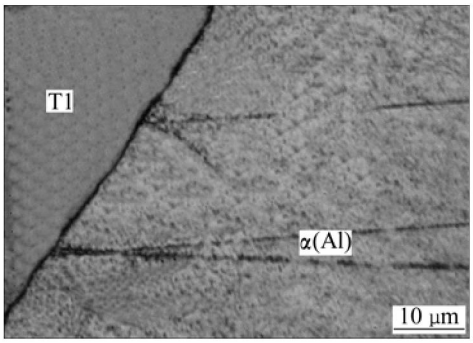

Fig.10 Optical micrograph of simulated Al alloy containing T1 particle

Fig.11. It is clearly seen that corrosion occurs on the T1 particle. Meanwhile, a groove is found on α(Al) around the simulated T1 particle, indicating that corrosion also occurs on α(Al). It should be noticed that the corrosion of α(Al) occurs at the adjacent periphery of the T1 particle and no obvious corrosion is observed far from the T1 particle. Therefore, the corrosion of α(Al) at the adjacent periphery of the T1 particle should be caused by galvanic corrosion at a later stage of immersion. This phenomenon is consistent with the coupling test. According to the coupling behavior of T1-α(Al) system

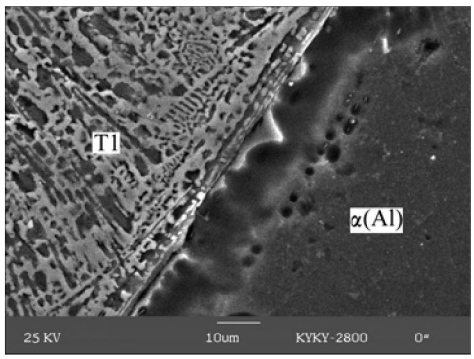

Fig.11 Corrosion morphology of simulated Al alloy immersed in 3.5% NaCl solution for 12 h

in 3.5% NaCl solution, it is known that the precipitate of T1 is changed gradually from anode to cathode, resulting in the anodic dissolution and corrosion of α(Al) at a later stage.

Based on the above results, a dynamic conversion corrosion mechanism associated with the precipitate of T1 in Al-Li alloys can be advanced here. At the beginning, the precipitate of T1 is anodic to the alloy base. Anodic dissolution and corrosion occur on its surface. However, during its corrosion process, its potential moves to a positive direction with corrosion time, due to the preferential dissolution of Li and the enrichment of Cu. As a result, the precipitate of T1 becomes cathodic to the alloy base, leading to the anodic dissolution and corrosion of the alloy base at its adjacent periphery at later stage. During the corrosion of the alloy base, other T1 precipitate will be exposed to the corrosion medium, and the above process will be repeated. So, the corrosion associated with the precipitate of T1 should be caused by the alternate anodic dissolution of the T1 precipitate and the alloy base at its adjacent periphery.

4 Conclusions

1) At the beginning of immersion in 3.5% NaCl solution, the precipitate of T1 is anodic to α(Al) and more susceptible to corrosion than α(Al).

2) As the precipitate of T1 is coupled with α(Al) in 3.5% NaCl solution, its potential moves to a positive direction. As a result, the precipitate of T1 becomes cathodic to α(Al), leading to the anodic dissolution and corrosion of α(Al).

3) There exists a dynamic conversion corrosion mechanism associated with the precipitate of T1 in Al-Li alloys. During the corrosion process, the precipitate of T1 is changed gradually from anode to cathode. It is suggested that the corrosion associated with the precipitate of T1 in Al-Li alloys is caused by the

alternate anodic dissolution of the T1 precipitate and the alloy base at its adjacent periphery.

References

[1] LI Jin-feng, ZHANG Zhao, CHENG Ying-liang, CAO Fa-he, ZHANG Jian-qing, CAO Chu-nan. Effect of aging state on localized corrosion of Al-4.0Cu-1.0Li-0.4Mg-0.4Ag-0.14Zr alloy in 3.0% NaCl solution [J]. The Chinese Journal of Nonferrous Metals, 2002, 12(5): 967−971. (in Chinese)

[2] CUI Wen-fang, SUN Qiu-xia, CUI Jian-zhong. Study corrosion resistance of 01420 Al-Li alloy [J]. Rare Metal Materials and Engineering, 1995, 24(2): 40−44. (in Chinese)

[3] WEI Xiu-yu, TAN Cheng-yu, ZHENG Zi-qiao, LI Jin-feng. Influence of aging on corrosion behavior of 2195 Al-Li alloy [J]. The Chinese Journal of Nonferrous Metals, 2004, 14(7): 1195−1200. (in Chinese)

[4] ZHANG Yun, ZHU Zi-yong, WANG Zheng-fu. Intergranular and exfoliation corrosion behavior of AI-Li alloy [J]. Journal of Chinese Society of Corrosion and Protection, 1992, 12(2): 180−184. (in Chinese)

[5] BUCHHEIT R G, MORAN J P, STONER G E. Electrochemical behavior of $T_1(Al_2CuLi)$ intermetallic compound and its role in localized corrosion of Al-2%Li-3%Cu alloys [J]. Corrosion, 1994, 50(2): 120−130.

[6] BUCHHEIT R G, MORAN J P, STONER G E. Localized corrosion behavior of alloy 2090—the role of microstructure heterogeneity [J]. Corrosion, 1990, 46(8): 610−617.

[7] KUMAI C, KUSINSKI J, THOMAS G. Influence of aging at 200 ℃ on the corrosion resistance of Al-Li and Al-Cu-Li alloys [J]. Corrosion, 1989, 45(4): 294−302.

[8] KUMAR K S, BROWN S A, PICKENS J R. Microstructural evolution during aging of an Al-Cu-Li-Ag-Mg-Zr alloy [J]. Acta Mater, 1996, 44(5): 1899−1915.

[9] NISKANEN P, SANDERS T H, KINKER J G. Corrosion of aluminium alloys containing lithium [J]. Corrosion Science, 1982, 22(4): 283−304.

[10] BUCHHEIT R G, GRANT R P, HLAVA P F, MCKENZIE B, ZENDER G L. Local dissolution phenomena associated with S phase (Al_2CuMg) particles in aluminium alloy 2024-T3 [J]. J Electrochem Soc, 1997, 144(8): 2621−2128.

[11] ZHU D Q, VAN OOIJ W J. Corrosion protection of AA 2024 T3 by bis-[3-triethoxysilyl]propy1]tetrasulfide in neutral sodium chloride solution (Part 1): Corrosion of AA2034-T3 [J]. Corrosion Science, 2003, 45(10): 2163−2175.

[12] SHAO M H, FU Y, HU R G, LIN C J. A study on pitting corrosion of aluminium alloy 2024-T3 by scanning micro-reference electrode technique [J]. Materials Science and Engineering A, 2003, A344(1−2): 323−327.

[13] LI J F, ZHENG Z Q, JIANG N, TAN C Y. Study on localized corrosion mechanism of 2 × × × series Al alloy containing $S(Al_2CuMg)$ and $\theta'(Al_2Cu)$ precipitates in 4.0% NaCl solution at pH6.1 [J]. Materials Chemistry and Physics, 2005, 91(2−3): 325−329.

[14] MIZUNO K, NYLUND A, OLEFJORD I. Surface reactions during pickling of an aluminum-magnesium-silicon alloy in phosphoric acid [J]. Corrosion Science, 2001, 43(2): 381−396.

[15] HUANG B P, ZHENG Z Q. Precipitation kinetics of an Al-4.01Cu-1.11Li-0.39Mg-0.19Zr -0.11Ti alloy [J]. Script Materialia, 1998, 38(4): 611−616.

(Edited by YUAN Sai-qian)